Code Based Design vs. Performance Based Design

A.M. Puthanpurayil,
Beca Ltd., Wellington, New Zealand.

R. Jury
Beca Ltd., Wellington, New Zealand.

J. Hooper
Magnusson Klemencic Associates, Seattle, USA.

A.J Carr
University of Canterbury, Christchurch, New Zealand.

ABSTRACT

Modern day design codes are the result of six decades of seismic engineering developments, most of which have been focused on elastic modal methods. Modal methods are strictly not applicable to inelastic systems and hence the adaptation of modal methods to seismic engineering has demanded that assumptions be made on fundamental aspects and restrictions be made on designs to provide confidence that the systems developed could be expected to perform well in an earthquake. These assumptions and restrictions lead to simple prescriptive rules which in the present day forms the backbone of most prescriptive code procedures. Although some of these assumptions have no physical/ mathematical justification other than "mathematical convenience", the methods have become so ingrained in common day design practice that practitioners believe they provide the ultimate truth and demands that all designs must ultimately follow these simple rules. This thinking creates a huge impediment in the implementation of true performance based seismic design (PBSD), because it fundamentally defeats the purpose of the process of PBSD. In comparison to code-based design, where once the prescriptive rules are satisfied, it is believed the system will perform adequately In true PBSD, the target or demonstrated performance should drive the design. This focus of true PBSD requires the design be proven to satisfy the laws of physics rather than simple prescriptive rules. In this paper, using complex modal analysis, we discuss the issues with the pseudo procedure in prescriptive codes and the impediments in implementing "true" PBSD in a professional community so wedded to prescriptive procedures. Through numerical examples, it is shown that a "true" PBSD design *does not need to* demonstrate compliance by traditional prescriptive approaches adopted in the code.

1 INTRODUCTION

Due to the increase in estimates of seismic hazard (e.g. in Wellington the hazard goes up by a factor of 2), and the cost of the past earthquakes, (e.g. Christchurch earthquake series cost >NZD $ 45 billion, about 20% New Zealand's GDP), modern day seismic design strategies for highly seismic regions like Wellington in New Zealand are slowly shifting towards performance-based approaches.

In a performance-based approach, the design is completed to achieve a certain set of performances in the future earthquakes. Unlike the prescriptive code methods, the performance-based design approaches require the design to demonstrate that the targeted performances are achieved. In this context, a "true" Performance-Based Seismic Design (PBSD) (as used in this paper) refers to the designs which are shown to have achieved compliance through rigorous nonlinear time history analysis (NLTHA).

In practice, generally the PBSD first starts with the prescriptive code approach. Once the design satisfies the code clauses. it is subjected to NLTHA for evaluating the performance. If all the performance estimates are satisfactory, then the design is deemed acceptable and, if not, it is revised. So, in practice, this might result in several iterations of the design. Through this process of following the prescriptive procedure (code-based approach) in general practise is a matter of convenience. The majority of the profession seems to believe that to provide an acceptable design, the prescriptive requirements must be satisfied. This presents a huge impediment in the implementation of "true" PBSD in practice.

In this paper, we demonstrate using *nonclassical modal analysis* that for a "true" PBSD carried out using NLTHA, there appears to be no need to satisfy the prescriptive rules of a code-based design. We also demonstrate that the prescriptive code-based approaches using classical modal methods are, at most, a convenience that has limited mathematical or physical justification when applied to an inelastic system. To show this, we begin the paper with a section describing how inelasticity actually happens in the structure; the next section summarises very recent work by Carr et al. 2024 where the concept of complex modes is introduced; the following next section introduces the concept of complex participation factor, effective mass of an inelastic system and migrating base shears; section 5 uses two case study structures to demonstrate the effects described in sections 3 and 4; section 6 provides conclusions the authors have reached.

2 HOW IS INELASTICITY EXHIBITED IN REAL STRUCTURES?

Inelastic excursions are inevitable in the response of structures subjected to high seismic loading. A well-designed structure tends to develop nonlinear hinges at selected locations as a means for dissipating the seismic energy. Figure 1 (Sharpe 1974) illustrates the snapshots of these concentrated hinge occurrences in a 2D frame structure during different instances of time in a NLTHA. The frame is subjected to the classic El Centro earthquake. The black dots in Figure 1 depict the plastic hinges and the numerical value below each frame depicts the time (i.e., 4.89 means 4.89 seconds). It can be seen that there is no definite pattern in which the hinges appear and disappear and this is a function of the specific characteristics of the structure and the incoming ground motion dynamics.

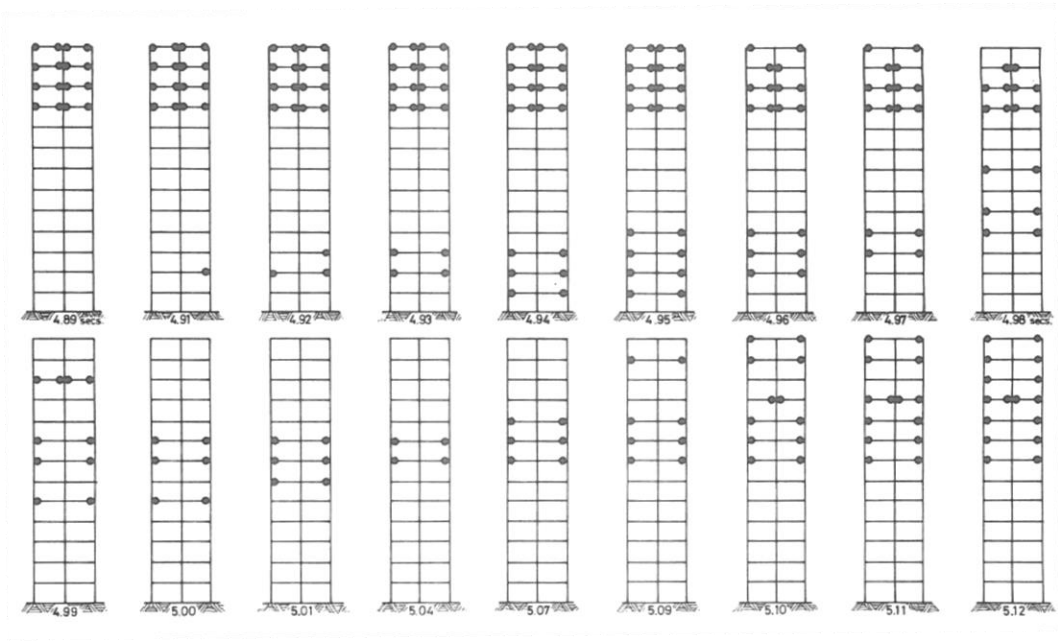

Figure 1: Hinge migration in a multi-storey structure when subjected to El-Centro May 1940

What Figure 1 does not illustrate is the amount of incurred ductility or what degree of deformation is being exhibited by individual hinges. In other words, when inelastic excursions happen at certain points as illustrated by Figure 1, depending on the structural dynamics and the ground motion interaction dynamics, the incurred ductility/deformation in individual hinges will vary quite remarkedly. The direct implications of this variability of deformations in the local hinges on the whole system will be that, at every time step, there will be differences in the deformation pattern and amplitude exhibited by the global mode. In other words, this means at each time step, depending on the inelasticity, the system has a completely different set of basis vectors or eigen modes. The next section will try to illustrate this in more detail.

3 HOW DOES THE DYNAMICS OF THE STRUCTURE CHANGE WHEN INELASTICITY OCCURS?

In section 2, it was shown that inelasticity may not occur uniformly and may have highly coupled spatio-temporal variance in the behavior, even in reasonably simple structural forms. The pertinent question is, what does this spatio-temporal variance in the behavior mean to the overall system dynamics? To answer this, a detail study was conducted by Carr et al. (2024) using complex modal-domain-based-dynamics using a simple four storey shear frame as a case study. The key outcomes of the study are summarised as follows:

- When system goes inelastic, damping is no longer proportional and the assumptions implied in the classical modal dynamics are violated, invalidating the response spectrum approach.
- Mode shapes change when system becomes inelastic and is complex in nature with appearance of imaginary components resulting in phasing effects (Refer Figures 2-4).
- Natural frequencies are complex after system becomes inelastic.
- Modal damping ratios become complex numbers when a system becomes inelastic.

More details on each of these outcomes are available in the paper. Although each of these outcomes illustrate the violation of classical modal dynamics, from a design point of view, the net effect is felt in the gross violation of the physics in the inherent assumption of the simplification of a MDOF system to a SDOF system. In other words, when the system goes inelastic there is effectively a different base shear that is felt by the system in different modes at every time step. Alternatively, what happens is, there will be modal mass migration and

hence base shear migration or fluctuations between modes. In this paper a mathematical illustration is presented on this effective modal base shear which is an extension of the work done by Carr et al. (2024). Section 6 demonstrates this phenomenon of modal base shear migrations through two case studies.

Before delving into the mathematical basis, Figures 2-4 presents the proportional and nonproportional (complex) mode shapes. A nonproportional/complex mode shape (blue) appears when the system goes inelastic and as depicted in the Figures 2-4, every degree of freedom in the mode does not reach the maximum modal displacement at the same instant; in other words, they exhibit phasing effects.

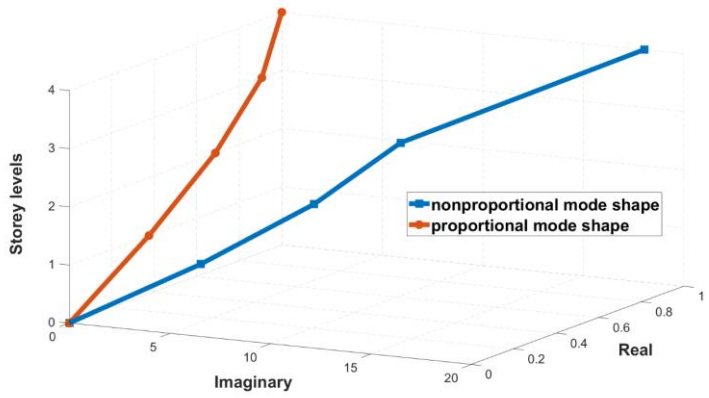

Figure 2: Elastic and inelastic first mode of a four-storey shear frame (Carr et al. 2024)

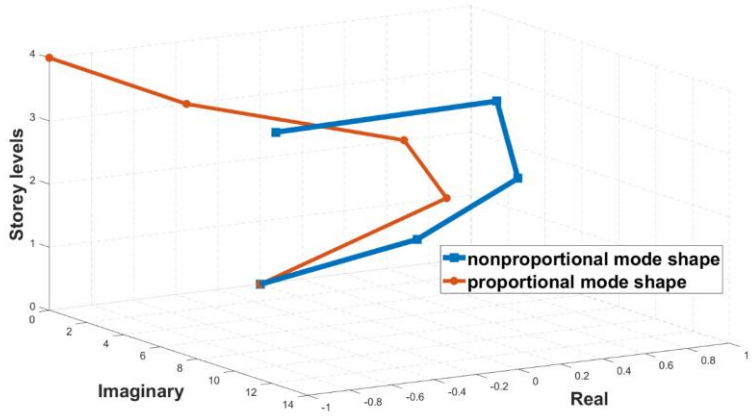

Figure 3: Elastic and inelastic second mode of a four-storey shear frame (Carr et al. 2024)

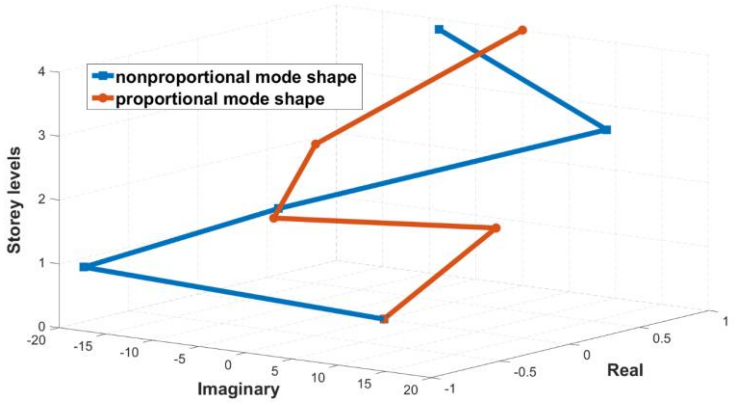

Figure 4: Elastic and inelastic third mode of a four-storey shear frame (Carr et al. 2024)

The pertinent question is *what will be the implications of this phenomenon of appearance of these complex modes for the common modal based design process adopted in the code?* Alternatively, *does the appearance of complex modes result in an error in the normal spectral based design process?*

As can be seen from Figures 2-4, when the system goes inelastic, the mode shapes are no longer the same as an elastic system. This aspect has huge effect on the prescriptive procedures followed by the codes as the underlying principle followed by all major codes is that *mode shape remains the same*. However, when the system goes inelastic, that is not true. Sections 4 and 5 demonstrate the implication of this aspect by reflecting the changes in the computed effective complex modal mass and hence the structures base shears.

4 CONCEPT OF COMPLEX MODE PARTICIPATION FACTOR, EFFECTIVE MASS AND FLUCTUATING MODAL BASE SHEARS

As described in the previous section, when the structure goes nonlinear the system becomes nonproportional which means the classical real modes no longer exist. This now calls for a nonclassical approach when applying modal analysis. In this section a brief description of the nonclassical modal analysis is given and a new concept of a complex mode participation factor and associated effective modal mass and base shear using complex modes are described. *Readers who are not interested in the mathematical derivations may skip this section without any discontinuity to the reading*.

Classical equation of motion for a structural system subjected to earthquake loading is given as,

$$M\ddot{u}(t) + C\dot{u}(t) + Ku(t) = -MR\ddot{u}_g(t) \quad (1)$$

Here, M, C and K are the mass, damping and stiffness matrices, respectively. $f(t)$ is the force vector varying with time and, in the case of earthquake loading, this becomes $-MR\ddot{u}_g(t)$ where $\ddot{u}_g(t)$ is the ground-motion acceleration record, R is the directionality influence vector and (t) indicates variation of the quantity with time. $\ddot{u}, \dot{u}$ and u represent the relative acceleration, velocity, and displacements, respectively.

For the structure presented in equation (1) to have *normal modes* or *classical modes*, the Caughey criterion needs to be satisfied. The Caughey criterion (Caughey & Kelly 1965) states that, for normal modes to exist,

$$KM^{-1}C = CM^{-1}K \quad (2)$$

In the case of equation (2), when structure goes nonlinear, this does not hold true, and hence the damping becomes non-proportional; in other words the original basis vectors (elastic mode shapes) cannot diagonalize the "M-C-K" matrices.

For a proportionally damped structure the mode shapes are identical to those of the undamped structure and only the natural frequencies are modified by the damping. This is the assumption in all code-based design methods. If the structure exhibits non-proportional damping, the eigen-problem is non-symmetric so that the natural frequencies, damping ratios and mode shapes may be complex numbers.

To understand physically the effects of non-proportionality, let's consider the homogenous monic form of equation (1):

$$I\ddot{u}(t) + M^{-1}C\dot{u}(t) + M^{-1}Ku(t) = 0 \tag{3}$$

Equation (3) is further transformed as:

$$M^{-1/2}MM^{-1/2}M^{1/2}\ddot{u}(t) + M^{-1/2}CM^{-1/2}M^{1/2}\dot{u}(t) + M^{-1/2}KM^{-1/2}M^{1/2}u(t) = 0 \tag{4}$$

Assigning the following:

$$\left.\begin{aligned} y(t) &= M^{1/2}u(t) \\ \hat{C} &= M^{-1/2}CM^{-1/2} \\ \hat{K} &= M^{-1/2}KM^{-1/2} \end{aligned}\right\} \tag{5}$$

Equation (3) becomes:

$$I\ddot{y}(t) + \hat{C}\dot{y}(t) + \hat{K}y(t) = 0 \tag{6}$$

Now, in the modal domain:

$$y(t) = \Phi_n q(t) \tag{7}$$

Φ_n represents the normal mode obtained by ignoring the damping term or in other words the basis vectors only considering the "M and K" matrices. Substituting equation (7) in equation (6) and pre-multiplying by ${\Phi_n}^T$, we get:

$$\begin{bmatrix} 1 & \cdots & 0 \\ \vdots & \ddots & \vdots \\ 0 & \cdots & 1 \end{bmatrix}\{\ddot{q}(t)\} + \left[{\Phi_n}^T\hat{C}\Phi_n\right]\{\dot{q}(t)\} + \begin{bmatrix} \widehat{k_1} & \cdots & 0 \\ \vdots & \ddots & \vdots \\ 0 & \cdots & \widehat{k_n} \end{bmatrix}\{q(t)\} = 0 \tag{8}$$

If the damping is proportional, the second matrix term on the left-hand side should also have a diagonal form that de-couples the entire MDOF into a series of SDOFs. This is not the case when the structure goes inelastic as the Caughey criterion, given in eq.(2) is generally violated and the damping non-proportionality phenomenon is exhibited. *In other words, systems with non-proportional damping will have off-diagonal terms which are of considerable magnitude preventing the above-mentioned de-coupling of the entire MDOF structure into a series of SDOFs using normal modes*.

Therefore, an alternative treatment with a damped eigen-decomposition needs to be undertaken. The eigen decomposition of the $M - C - K$ structure is performed through a state-space formulation. Readers can refer to Hurty & Rubinstein (1964) for more details.

$$\begin{Bmatrix} \ddot{u}(t) \\ \dot{u}(t) \end{Bmatrix} = \begin{bmatrix} -M^{-1}C & -M^{-1}K \\ I & 0 \end{bmatrix}\begin{Bmatrix} \dot{u}(t) \\ u(t) \end{Bmatrix} \tag{9}$$

$$\left.\begin{gathered}\begin{bmatrix}-M^{-1}C & -M^{-1}K\\ I & 0\end{bmatrix}=\Phi\Lambda\Phi^{-1}\\ \Phi=\begin{bmatrix}\Phi_c\Lambda_c & \Phi_c^*\Lambda_c^*\\ \Phi_c & \Phi_c^*\end{bmatrix}\\ \Lambda=\begin{bmatrix}\Lambda_c & 0\\ 0 & \Lambda_c^*\end{bmatrix}\\ \Lambda_c=\begin{bmatrix}\lambda_{c,1} & \cdots & 0\\ \vdots & \ddots & \vdots\\ 0 & \cdots & \lambda_{c,n}\end{bmatrix}\end{gathered}\right\} \quad (10)$$

Here, $\lambda_{c,i}$ are the eigen values and Φ_c is the complex mode shape matrix for $the\ M-C-K$ system.

To further investigate the concept of non-proportionality, let's rewrite equation (18) in the complex modal domain.

Assume:

$$y(t)=\Phi_c e^{\lambda_c t} \quad (11)$$

Substituting equation (13) into equation (8) and pre-multiplying by ${\Phi_n}^T$, we get:

$${\Phi_n}^T\Phi_c{\Lambda_c}^2+{\Phi_n}^T\hat{C}\Phi_c\Lambda_c+\Omega^2\Phi_c=0 \quad (12)$$

where:

$$\Omega^2=diag\left(\omega_{ni}^2\right) \quad (13)$$

and is the eigen value matrix of $\widehat{K}$. For the *i*th mode, equation (15) may be re-written as:

$$\omega_i^2+\omega_i\frac{(\phi_{n,i}^T\hat{C}\phi_{c,i})}{\phi_{n,i}^T\phi_{c,i}}+\omega_{n,i}^2=0 \quad (14)$$

Equation (16) may be re-written as:

$$\omega_i^2+\omega_i\left(c_{ii}+\frac{(\phi_{n,i}^T\hat{C}\phi_{c,i})}{\phi_{n,i}^T\phi_{c,i}}\right)+\omega_{n,i}^2=0 \quad (15)$$

Where c_{ii} represents the real component of the damping coefficient and $\frac{(\phi_{n,i}^T\hat{C}\phi_{c,i})}{\phi_{n,i}^T\phi_{c,i}}$ is the imaginary component of the damping coefficient.

Since $\phi_{c,i}$ is a complex value, we can say that:

$$\frac{1}{2\omega_{n,i}}\left(c_{ii}+\frac{(\phi_{n,i}^T\hat{C}\phi_{c,i})}{\phi_{n,i}^T\phi_{c,i}}\right)=\xi+i\gamma \quad (16)$$

In the spirit of the damping ratio in classical modal analysis, Equation (16) describes the complex damping ratio. Alternatively, Equation (16) may be viewed as a combination of the classical damping ratio (which is real) and an imaginary damping ratio component which reflects the other mode effects on the damping ratio. In other words, these so-called other mode effects create the phenomenon of non-proportionality. According to Liang and Lee (1991), this is called the modal energy transfer ratio which reflects the energy transfer to other modes.

If $\gamma \neq 0$, the complex mode exists, and hence complex mode participation factor also exists which means the effective mass participating ratio will be different to what is normally computed using classical modes. How to compute the complex mode participation factor, state space formulation, is revisited.

Eq. (1) is rewritten in state space format as,

$$\dot{y} = Ay + BZ(t) \tag{17}$$

Where,

$$\left.\begin{aligned} A &= \begin{bmatrix} M^{-1}C & -M^{-1}K \\ I & 0 \end{bmatrix} \\ B &= \begin{bmatrix} -R \\ 0 \end{bmatrix} \\ Z &= \begin{Bmatrix} \ddot{u}_g(t) \\ 0 \end{Bmatrix} \\ y &= \begin{Bmatrix} \dot{u} \\ u \end{Bmatrix} \end{aligned}\right\} \tag{18}$$

For simplicity, if we only adopt the homogenous part of eq. (17) we get,

$$x = \Phi_c e^{\lambda_c t} \tag{19}$$

Now on complex eigen-decomposition, we get,

$$\Phi_c = \begin{Bmatrix} \lambda_c \phi_c \\ \phi_c \end{Bmatrix} \tag{20}$$

Since for the specific instant in time system is represented by the secant stiffness, it is linear and the response at that instant is given as,

$$x(t) = \sum_{i=1}^{N} \phi_{ci} e^{\lambda_{ci} t} + \sum_{i=1}^{N} \tilde{\phi}_{ci} e^{\tilde{\lambda}_{ci} t} \tag{21}$$

Here $\tilde{\phi}_{ci}$ indicates the complex conjugate and similarly for the $\tilde{\lambda}_{ci}$ as well.

Applying Laplace to eq. (17), we get,

$$\left[s\begin{Bmatrix} sX(s) \\ X(s) \end{Bmatrix} - \quad A\begin{Bmatrix} sX(s) \\ X(s) \end{Bmatrix} \right] = \begin{Bmatrix} M^{-1}\ddot{u}_g(s) \\ 0 \end{Bmatrix} \tag{22}$$

Where "s" is the Laplace variable and $X(s)$ and $\ddot{u}_g(s)$ are the transformation of $x(t)$and $\ddot{u}_g(t)$.

Applying eq. (21) in eq. (22) and doing standard mathematical manipulations in Laplace domain, the response of the i^{th} mode intime domain maybe given as,

$$x_i(t) = \mathcal{L}^{-1}\{-H_i(s)\ddot{u}_g(s)\} \tag{23}$$

where,

$H_i(s) = \frac{X(s)}{\ddot{u}_g(s)}$ & $\mathcal{L}^{-1}$ denotes inverse Laplace. (24)

So now in time domain, for lightly damped systems, we get,

$$x_i(t) = 2\omega_i(\xi_i \Phi_i - \Psi_i)y(t) + 2\Phi_i \dot{y}(t) \tag{25}$$

Here, Φ_i and Ψ_i are the real and imaginary part of the product of the complex mode shape and the accompaniment matrix. Now taking motivation from classical modal dynamics, expressing maximum $\dot{y}(t)$ in an approximate sense as,

$$\dot{y}(t) = \omega_i cos\theta y_{max} \tag{26}$$

now eq. (25) reduces to,

$$x_{i,max} = 2\omega_i(\xi_i \Phi_i - \Psi_i)y_{max} + 2\Phi_i \omega_i cos\theta y_{max} \tag{27}$$

Where θ represents angle so that displacement reaches peak value . On further mathematical manipulation of eq. (27), (for details readers may refer to Hurty and Rubinstein), we get,

$$x_{i,max} = 2\omega_i\{(-\xi_i\Phi_i + \Psi_i) + 0.4\Phi_i\}y_{max} \quad (28)$$

Now taking motivation from classical modal dynamics, the complex participation factor maybe approximated as,

$$\Gamma_i \cong \frac{2\omega_i\{(-\xi_i\Phi_{ij}+\Psi_{ij})+0.4\Phi_{ij}\}}{\breve{\Phi}_{ij}} \quad (29)$$

where,

$$\breve{\Phi}_{ij} = \frac{|\Phi_i|}{\Phi_{ni}} sgn(\Phi_{ni}) \quad (30)$$

Now motivated from classical modal dynamics, i^{th} participating complex mass ratio is given as,

$$PF_{m,i} = \frac{Re\{(\Gamma_i)^2\}}{\sum_{j=1}^{N} m_j} \quad (31)$$

The corresponding i^{th} mode complex base shear may be given as,

$$V_{B,i} = PF_{m,i} \sum_{j=1}^{N} m_j S_{a,i} \quad (32)$$

where $S_{a,i}$ is the spectral ordinate corresponding to the period of i^{th} mode.

Eq. (31) and eq. (32) give a means to estimate the effective mass and the effective base shear for an inelastic structure using complex modal mechanics. The significance of equations. 31&32 is that as the inelasticity happens the effective modal mass and hence the base shear changes for individual modes resulting in different member actions and deformations across the structure.

5 NUMERICAL CASE STUDIES

This section investigates the aspect of change in effective modal mass and hence base shear migrations during inelastic excursions discussed in the previous sections. Two simple case studies are used to demonstrate this: a two-storey structure and a six-storey structure. Figure 1 shows how hinges migrate in a real structure. In every time step, the structure has a different hinge migration up the height illustrating the fact that it exhibits different states of inelasticity. In the present examples the inelastic states denoted as inelastic 1,2,3,4 try to mimic these time snaps described in Figure 1.

5.1 Two-storey structure

Figure 5 illustrates a two storey structure with $m_1 = 2.0tonnes$, $m_2 = 2.5tonnes$, $k_1 = 850kN/m$ and , $k_2 = 750kN/m$. For simplicity the Rayleigh damping matrix is adopted for the c_1& c_2 coefficients.

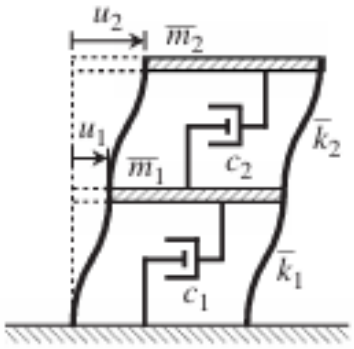

Figure 5: Two-storey shear frame system

Table 1 computes the participating mass ratios using effective mass computed using eq. 31. In the purest sense, eq. 31 is only applicable to elastic systems with nonproportional damping. Table 1 is therefore computed using the instantaneous secant stiffness matrix, because at every instant of inelasticity, the physical structure in reality responds in its secant stiffness state. In other words, for every instant of inelasticity (Figure 1), there is a set of basis vectors (complex eigen vectors) which results in the dynamic responses exhibited by the structure.

Table 1 Migrating mass participating ratios for different states of inelasticity

Mode	Elastic	Inelastic 1	Inelastic 2	Inelastic 3	Inelastic 4
1	93%	98%	72%	78%	96%
2	7%	2%	28%	22%	4%

In Table 1, Inelastic 1 to 4 describes different states of inelasticity, with inelastic 1 being first storey inelastic and the rest elastic, inelastic 2 being the top storey inelastic and inelastic3 & 4 being both storeys in different states of inelasticity. In each of these states, secant stiffnesses are calculated, and using the complex basis set out in section 4 the values in

Table 1 are computed using eq. 31.

As can be seen from Table 1, the structure exhibits different mass participation ratios at different stages of inelasticity. This is a very important observation as even a simple 2-storey structure exhibits inelastic participating mass migrations. The differences in the participation in different modes in different inelastic states can be very different to the elastic state (e.g., the second mode participation in inelastic state 2 is about 400% more than in the elastic state). This simply means at that specific instant; the second mode base shear is at the least 400% different to what is being estimated from an elastic analysis. *This results in larger member forces and deformation responses which is the main reason why structures designed to the codes may sometimes exhibit very different responses when evaluated with nonlinear time history analysis*.

5.2 Six-storey structure

Figure 6 illustrates a six-storey structure with uniform masses m_i $(i = 1 \ldots 6)$ of 80 tonnes and stiffness k_i $(i = 1 \ldots 6)$ of 4×10^7 N/m. For simplicity Rayleigh damping matrix is adopted for the

c_i $(i = 1 \ldots 6)$ coefficients.

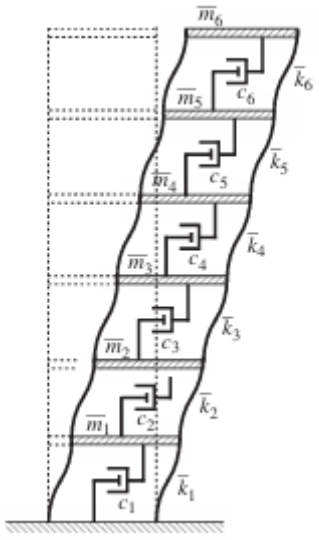

Figure 6: Six-storey shear frame system

Table 2 Migrating mass participating ratios for different states of inelasticity

Mode Number	Elastic	Inelastic 1	Inelastic 2	Inelastic 3	Inelastic 4
1	87%	82%	97%	68%	76%
2	9%	8%	2.5%	29%	15%
3	3%	5%	0.5%	1%	8%

Table 2 computes the participating mass ratios using the effective mass computed using eq. 31. Similar to section 5.1, Table 2 is computed using the instantaneous secant stiffness matrices.

Inelastic 1…4 states in Table 2 exhibits different states of inelasticity, with inelastic 1 being first storey inelastic and rest elastic, inelastic 2 being top storey inelastic and inelastic 3 & 4 being both storeys in different state of inelasticity. In each of state, secant stiffnesses are calculated and the Table 2 is computed using eq. 31.

As can be seen from Table 2, the structure exhibits different mass participation ratios at different stages of inelasticity. This is a very important observation that is similar to the 2-storey structure; the 6-storey structure also exhibits inelastic participating mass migrations. The differences in the participation in different modes in different inelastic state can be very different to the elastic state, for example, the second mode participation in inelastic state 3 is about 320% more than in the elastic state. This simply means at that specific instance, the second mode base shear is at the least 320% different to what is being estimated from an elastic analysis.

This suggests that the prescriptive pseudo spectral approach adopted in codes does not necessarily reflect the real dynamics as exhibited by the inelastic structure and the actions associated with it.

The phenomenon of modal mass migrations and the base shear migrations are automatically accounted for in a NLTHA analysis. Hence the authors believe that in a “true” PBSD design showing compliance through NLTHA, where all the inelastic actions are reliably estimated, there is no need to show compliance through the prescriptive procedures as outlined in the code.

6 CONCLUSIONS

Using complex modal analysis, the paper discusses the issues associated with the prescriptive procedures adopted in the code approaches and the need for a *paradigm shift* in the design thinking by the profession. The concept of complex modal mass participation ratio is introduced and how to compute it is presented. It is shown through numerical examples that the common belief that a "true" PBSD design needs to demonstrate compliance through traditional prescriptive approaches adopted in the code is *completely unfounded*. The profession needs to recognize the superiority of the NLTHA methods over modal/spectral methods. We feel that these methods should be made the main compliance pathway and made mandatory for seismic design in regions with a likelihood of large ground shaking.

REFERENCES

1 Carr A.J., Puthanpurayil A.M, Sharpe RD, Jury R (2024). "*Structures incorporating damping devices: are we correct in our design thinking?"* Bulletin of New Zealand Society of Earthquake Engineering (in print)

2 Caughey, TK and Kelly, MEJ. (1965). "Classical Normal Modes in Damped Linear Dynamic Systems". *J. Appl. Mech*. Sep 1965, 32(3): 583-588.

3 Hurty, WC and Rubinstein, MF. "Dynamics of Structures", *Prentice-Hall, Englewood Cliffs N.J. 1964, 455p*

4 Liang, Z and Lee, GC. (1991). "Damping of Structures – Part 1: Theory of Complex Damping". *Technical Report NCEER-91-0004, October 10, 1991. University of Buffalo, NY. 248p.*

5 Sharpe RD (1974). "*The seismic response of inelastic structures*". PhD Thesis, Department of Civil Engineering, University of Canterbury, New Zealand, pp125.